Article

Electron-catalysed molecular recognition

https://doi.org/10.1038/s41586-021-04377-3

Received: 6 September 2021

Accepted: 22 December 2021

Published online: 9 March 2022

Check for updates

Yang Jiao[1,10], Yunyan Qiu[1,10], Long Zhang[1], Wei-Guang Liu[2], Haochuan Mao[1,3], Hongliang Chen[1,4,5], Yuanning Feng[1], Kang Cai[1,6], Dengke Shen[1,7], Bo Song[1], Xiao-Yang Chen[1], Xuesong Li[1], Xingang Zhao[1], Ryan M. Young[1,3], Charlotte L. Stern[1], Michael R. Wasielewski[1,3], R. Dean Astumian[8], William A. Goddard III[2]✉ & J. Fraser Stoddart[1,4,5,9]✉

Molecular recognition[1–4] and supramolecular assembly[5–8] cover a broad spectrum[9–11] of non-covalently orchestrated phenomena between molecules. Catalysis[12] of such processes, however, unlike that for the formation of covalent bonds, is limited to approaches[13–16] that rely on sophisticated catalyst design. Here we establish a simple and versatile strategy to facilitate molecular recognition by extending electron catalysis[17], which is widely applied[18–21] in synthetic covalent chemistry, into the realm of supramolecular non-covalent chemistry. As a proof of principle, we show that the formation of a trisradical complex[22] between a macrocyclic host and a dumbbell-shaped guest—a molecular recognition process that is kinetically forbidden under ambient conditions—can be accelerated substantially on the addition of catalytic amounts of a chemical electron source. It is, therefore, electrochemically possible to control[23] the molecular recognition temporally and produce a nearly arbitrary molar ratio between the substrates and complexes ranging between zero and the equilibrium value. Such kinetically stable supramolecular systems[24] are difficult to obtain precisely by other means. The use of the electron as a catalyst in molecular recognition will inspire chemists and biologists to explore strategies that can be used to fine-tune non-covalent events, control assembly at different length scales[25–27] and ultimately create new forms of complex matter[28–30].

Although the electron is an elementary particle, its impact on the reactivity of molecules is profound. In particular, the electron can act[17,18,31] as an effective catalyst to promote covalent reactions by lowering the energy barriers of bond formation. By treating (Extended Data Fig. 1) molecular recognition in an analogous fashion[32,33] to covalent reactions, we were led to the hypothesis that the electron can play an important role in catalysing the formation of supramolecular complexes. The strategy of electron catalysis is applicable to molecular recognition processes with certain essential features, that is, (1) there is at least one redox-active substrate capable of accepting (an) electron(s) rapidly, (2) there is an energy barrier that can be decreased by the injection of electron(s) and (3) there is a catalytic intermediate that is generated non-covalently from substrates and then transformed into the final product.

Accordingly, we selected (Fig. 1a) a host–guest system to demonstrate electron-catalysed molecular recognition. In this system, the host is $\mathbf{R}^{2(\bullet+)}$, which is a ring bearing two separate bipyridinium radical cations ($BIPY^{\bullet+}$). The dumbbell-shaped guest, $\mathbf{D}^{+(\bullet+)}$, comprises three parts: (1) a $BIPY^{\bullet+}$ unit in the middle, acting as the binding site for $\mathbf{R}^{2(\bullet+)}$ to form a trisradical complex[22] driven by radical-pairing interactions; (2) a 2,6-diisopropylphenyl group on one end of the dumbbell-shaped molecule to prevent the threading of the ring by steric hindrance; and (3) a 2,6-dimethylpyridinium (PY^{+}) cation on the other end, which—in conjunction with the positively charged $BIPY^{\bullet+}$ unit—fulfils the role of a switchable energy barrier. Preliminary investigations (Fig. 2a) have indicated that the passage of $\mathbf{R}^{2(\bullet+)}$ over the PY^{+} terminus of $\mathbf{D}^{+(\bullet+)}$ is very slow on account of strong Coulombic repulsion. The energy barrier resulting from this repulsive interaction, which depends on the numbers of charges on the host and guest, can be adjusted (Fig. 1a) by changing the redox states[34] of the bipyridinium units.

We propose (Fig. 1b) a design for electron-catalysed molecular recognition between $\mathbf{R}^{2(\bullet+)}$ and $\mathbf{D}^{+(\bullet+)}$. The catalysis is initiated by injection of an electron (step 1), giving rise to the reduction of one $BIPY^{\bullet+}$ radical cation in the system to its neutral state—namely, $BIPY^{(0)}$. Either $\mathbf{R}^{2(\bullet+)}$ or $\mathbf{D}^{+(\bullet+)}$ can accept (step 2) this electron to generate $\mathbf{R}^{\bullet+}$ or $\mathbf{D}^{+}$, respectively. As the electron is exchangeable, both the $\mathbf{R}^{\bullet+}$–$\mathbf{D}^{+(\bullet+)}$ couple and the $\mathbf{R}^{2(\bullet+)}$–$\mathbf{D}^{+}$ couple exist in the system. The energy barriers associated with the passage of the ring over the PY^{+} terminus were determined by quantum mechanical calculations (Supplementary Figs. 17 and 18) to be 9.3 and 8.8 kcal mol^{-1}, respectively. Both values are lower than the energy barrier (15.0 kcal mol^{-1}, Supplementary Fig. 16) associated with the direct binding between $\mathbf{R}^{2(\bullet+)}$ and $\mathbf{D}^{+(\bullet+)}$ without the additional electron. This result can be rationalized on the basis of the diminished Coulombic repulsion between the two molecules. The decrease in the energy barrier contributes to the rapid formation (step 3) of a $[\mathbf{D}\subset\mathbf{R}]^{+2(\bullet+)}$ bisradical complex, driven by a combination of radical-pairing and donor–acceptor interactions. This catalytic intermediate can be transformed to the final product, that is, the $[\mathbf{D}\subset\mathbf{R}]^{+3(\bullet+)}$ trisradical complex, concomitantly releasing (step 4) an electron to $\mathbf{R}^{2(\bullet+)}$ or $\mathbf{D}^{+(\bullet+)}$ to close the

[1]Department of Chemistry, Northwestern University, Evanston, IL, USA. [2]Materials and Process Simulation Center, California Institute of Technology, Pasadena, CA, USA. [3]Institute for Sustainability and Energy at Northwestern, Northwestern University, Evanston, IL, USA. [4]Stoddart Institute of Molecular Science, Department of Chemistry, Zhejiang University, Hangzhou, China. [5]ZJU-Hangzhou Global Scientific and Technological Innovation Center, Hangzhou, China. [6]Department of Chemistry, Nankai University, Tianjin, China. [7]Institutes of Physical Science and Information Technology, Anhui University, Hefei, China. [8]Department of Physics and Astronomy, University of Maine, Orono, ME, USA. [9]School of Chemistry, University of New South Wales, Sydney, New South Wales, Australia. [10]These authors contributed equally: Yang Jiao, Yunyan Qiu. ✉e-mail: wag@caltech.edu; stoddart@northwestern.edu

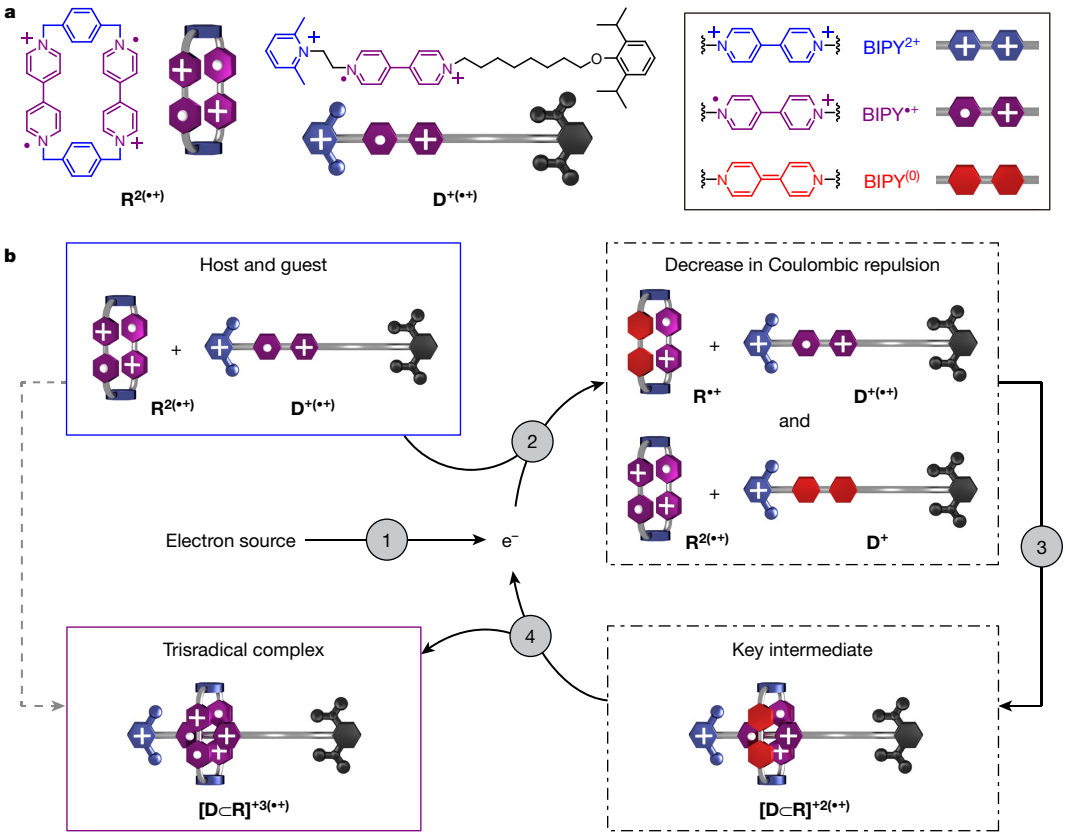

Fig. 1 | Design of an electron-catalysed molecular recognition process. **a**, Structural formulae and graphical representations of the host–guest system, which includes a macrocyclic host, $\mathbf{R}^{2(\bullet+)}$ and a dumbbell-shaped guest, $\mathbf{D}^{+(\bullet+)}$, investigated in this research. Electron catalysis arises from the fact that each BIPY unit in the system has three redox states, that is, dicationic (blue), radical cationic (purple) and neutral (red) states. **b**, Proposed mechanism for an electron-catalysed molecular recognition process. The direct (grey dashed arrow) formation of a $[\mathbf{D}\subset\mathbf{R}]^{+3(\bullet+)}$ trisradical complex from $\mathbf{R}^{2(\bullet+)}$ and $\mathbf{D}^{+(\bullet+)}$ is all but kinetically forbidden. The catalytic (black solid arrows) complexation comprises four steps, including one initiating step and three propagating steps. Step 1: the injection of an electron. Step 2: a single-electron reduction of either one of the BIPY$^{\bullet+}$ units in $\mathbf{R}^{2(\bullet+)}$ or the BIPY$^{\bullet+}$ unit in $\mathbf{D}^{+(\bullet+)}$. Step 3: the rapid formation of a $[\mathbf{D}\subset\mathbf{R}]^{+2(\bullet+)}$ bisradical complex, the key intermediate, favoured by a decrease in the Coulombic repulsion between the host and guest molecules. Step 4: the oxidation of the $[\mathbf{D}\subset\mathbf{R}]^{+2(\bullet+)}$ bisradical complex, producing a $[\mathbf{D}\subset\mathbf{R}]^{+3(\bullet+)}$ trisradical complex as the final product, while releasing an electron to close the catalytic cycle. Notably, although the electron is formally written into the catalytic cycle to highlight its role as a catalyst, such a representation does not imply the existence of a free electron during the catalytic process.

catalytic cycle. We anticipate that catalytic numbers of electrons can induce a marked acceleration of the molecular recognition between $\mathbf{R}^{2(\bullet+)}$ and $\mathbf{D}^{+(\bullet+)}$, even though this host–guest complexation is all but kinetically forbidden under ambient conditions.

To test the efficacy of this electron-catalysis approach, molecular recognition between $\mathbf{R}^{2(\bullet+)}$ and $\mathbf{D}^{+(\bullet+)}$ was carried out in an acetonitrile (MeCN) solution and monitored by ultraviolet (UV)/visible (Vis)/near-infrared (NIR) spectroscopy. The combination of only $\mathbf{R}^{2(\bullet+)}$ and $\mathbf{D}^{+(\bullet+)}$ brings about (Fig. 2a and Supplementary Fig. 10) little change in the absorption spectrum for at least 10 h, indicating that there is negligible formation of the $[\mathbf{D}\subset\mathbf{R}]^{+3(\bullet+)}$ trisradical complex. On addition of 4 mol% cobaltocene ($CoCp_2$, which is capable of transforming[34] BIPY$^{\bullet+}$ to BIPY$^{(0)}$), we observed (Fig. 2b) the appearance of a NIR absorption band (λ_{max} = 1,080 nm), which is characteristic[22] of the trisradical complex, accompanied by the decay in the absorption (λ_{max} = 600 nm) for the uncomplexed BIPY$^{\bullet+}$. This spectral change, which signifies the onset of molecular recognition, reaches a constant value in 70 min. Fitting (Supplementary Fig. 12) the data with a kinetic model for a second-order reversible reaction, the rate constant of this supramolecular process in the presence of 4 mol% $CoCp_2$ was determined to be 4.74 l mol^{-1} s^{-1}, showing a 640-fold acceleration compared to the rate constant (7.44 × 10^{-3} l mol^{-1} s^{-1}) observed in the absence of $CoCp_2$.

Increasing the amount of $CoCp_2$ from 4 to 8 mol% expedites (Fig. 2c) the molecular recognition process, rendering it complete in 10 min with a similar yield of the $[\mathbf{D}\subset\mathbf{R}]^{+3(\bullet+)}$ trisradical complex. Decreasing (Fig. 2d) the amount of $CoCp_2$ from 4 to 2 and then 1 mol% still promotes this process albeit at slower rates. Comparison (Fig. 2d) between the kinetic traces in the presence of 4 and 8 mol% $CoCp_2$ reveals the catalytic nature of the process: a small amount of $CoCp_2$ can accelerate the kinetics but has little influence on the thermodynamic equilibrium. Cyclic voltammetry measurements (Supplementary Fig. 13) confirm that the injection of electrons promotes the molecular recognition process, in which the reduction from BIPY$^{\bullet+}$ to BIPY$^{(0)}$, along with the reoxidation from BIPY$^{(0)}$ back to BIPY$^{\bullet+}$, proves to be indispensable for the formation of the $[\mathbf{D}\subset\mathbf{R}]^{+3(\bullet+)}$ trisradical complex on the timescale of the cyclic voltammetry experiments.

To investigate the mechanism of this molecular recognition, we performed (Fig. 3a) electron catalysis in a stepwise manner. In the first step, 1 molar equivalent (equiv) of $CoCp_2$ was added to the equimolar mixture of $\mathbf{R}^{2(\bullet+)}$ and $\mathbf{D}^{+(\bullet+)}$, leading to the instantaneous appearance (Fig. 3b, red line, and Supplementary Figs. 20–22) of a new, broad NIR absorption band centred at λ_{max} = 1,700 nm. This absorption band, which was different from that produced by the well-recognized [22] absorption (λ_{max} = 1,080 nm) for the trisradical complex, was ascribed to the $[\mathbf{D}\subset\mathbf{R}]^{+2(\bullet+)}$ bisradical complex. In the second step, further addition of excess of $\mathbf{D}^{+(\bullet+)}$ or $\mathbf{R}^{2(\bullet+)}$ into the system results in the transformation from the $[\mathbf{D}\subset\mathbf{R}]^{+2(\bullet+)}$ bisradical complex to the $[\mathbf{D}\subset\mathbf{R}]^{+3(\bullet+)}$ trisradical complex, as indicated by the shift of the absorption peak (Fig. 3b,

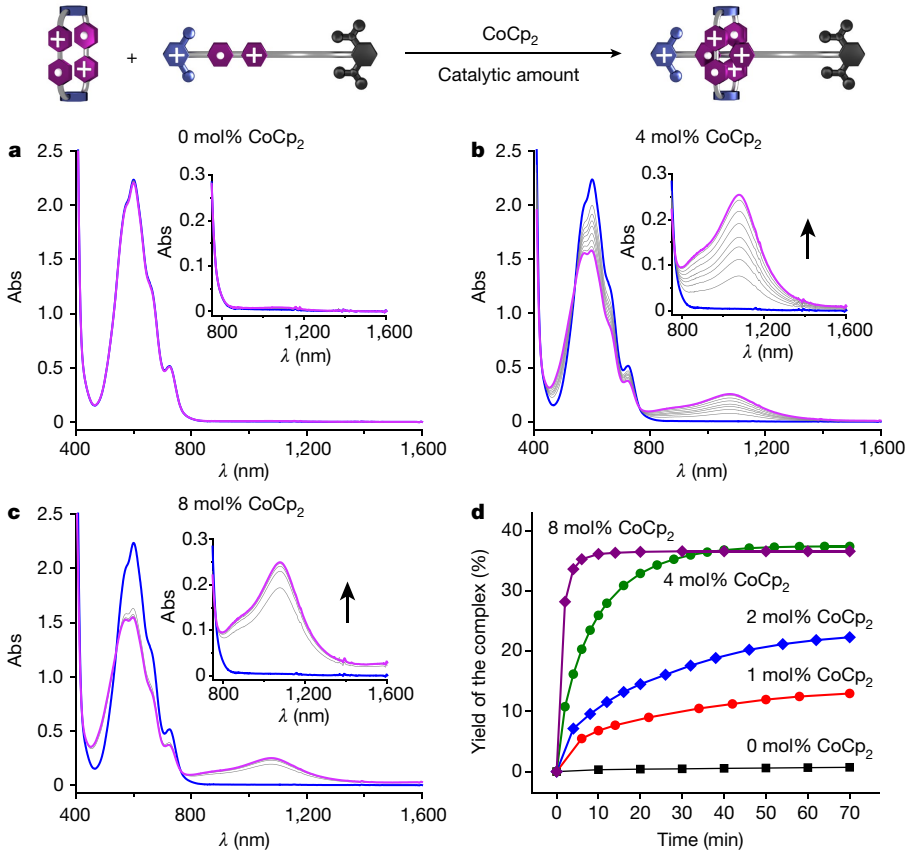

Fig. 2 | Molecular recognition accelerated by catalytic amounts of cobaltocene ($CoCp_2$). a–**c**, The evolution of UV/Vis/NIR spectra for a period of 70 min after combining equimolar amounts of $\mathbf{R}^{2(\bullet+)}$ and $\mathbf{D}^{+(\bullet+)}$ without added $CoCp_2$ (**a**) and with either 4 mol% $CoCp_2$ (**b**) or 8 mol% $CoCp_2$ (**c**). **d**, Kinetic traces for the host–guest complexation between $\mathbf{R}^{2(\bullet+)}$ and $\mathbf{D}^{+(\bullet+)}$ in the presence of different amounts of $CoCp_2$, obtained by plotting the yield of the $[\mathbf{D}\subset\mathbf{R}]^{+3(\bullet+)}$ trisradical complex against time. The concentrations of $\mathbf{R}^{2(\bullet+)}$ and $\mathbf{D}^{+(\bullet+)}$ were both fixed at 150 μM, and the concentration of $CoCp_2$ was set to be 0, 1.5, 3, 6 and 12 μM in different experiments. Abs, absorption.

blue line, and Supplementary Figs. 23 and 24) from 1,700 to 1,080 nm. We suggest that this bisradical complex serves as the key intermediate in the electron catalysis.

Further investigation of this intermediate was hindered because the combination of $\mathbf{R}^{2(\bullet+)}$, $\mathbf{D}^{+(\bullet+)}$ and $CoCp_2$ constitutes a complicated supramolecular system (Supplementary Fig. 25), involving multiple, interrelated host–guest complexation and electron transfer processes. A well-defined molecular system is therefore necessary to unravel the structure and properties of the bisradical complex. A [2]catenane ($\mathbf{Cat}^{6+}$)—in which a R^{4+} ring bearing two $BIPY^{2+}$ units and another ring containing one $BIPY^{2+}$ unit are mechanically interlocked—was synthesized[35] and used as a model compound. $\mathbf{Cat}^{6+}$ was first reduced to its trisradical tricationic state, $\mathbf{Cat}^{3(\bullet+)}$, followed by titration (Fig. 3c) with 1 equiv of $CoCp_2$. During the titration, the colour of the solution changed from purple to brown. Correspondingly, the characteristic absorption for the trisradical tricationic state (λ_{max} = 1,080 nm) was found to decrease gradually, accompanied by the elevation (Fig. 3d) of a new, red-shifted absorption band (λ_{max} = 1,640 nm) with isosbestic points at 506 and 1,219 nm. These observations indicate the quantitative transformation from $\mathbf{Cat}^{3(\bullet+)}$ to $\mathbf{Cat}^{2(\bullet+)}$. Notably, the absorption of $\mathbf{Cat}^{2(\bullet+)}$ is close to that of the $[\mathbf{D}\subset\mathbf{R}]^{+2(\bullet+)}$ bisradical complex, indicating the structural similarity of their chromophores. The electron paramagnetic resonance signal (Fig. 3e) of $\mathbf{Cat}^{2(\bullet+)}$ is nearly silent, supporting its diamagnetic nature in contrast with the paramagnetic nature of $\mathbf{Cat}^{3(\bullet+)}$.

Single-crystal X-ray diffraction analysis (Fig. 3f) verified the intercomponent binding within $\mathbf{Cat}^{2(\bullet+)}$, in which the R ring encircles the BIPY unit belonging to the other ring. The centroid-to-centroid distances between adjacent BIPY units in $\mathbf{Cat}^{2(\bullet+)}$ were found to be 3.17 and 3.31 Å, indicating[36] the existence of (1) a radical-pairing interaction between two adjacent $BIPY^{\bullet+}$ radical cations and (2) a donor–acceptor interaction between an electron-deficient $BIPY^{\bullet+}$ radical cation and an electron-rich $BIPY^{(0)}$ neutral unit. These interactions present in $\mathbf{Cat}^{2(\bullet+)}$ are also responsible for the formation of its non-interlocked counterpart, that is, the $[\mathbf{D}\subset\mathbf{R}]^{+2(\bullet+)}$ bisradical complex. Through the analysis of the model compound, we have identified the bisradical complex as the key intermediate during the electron-catalysed molecular recognition process, supporting strongly the mechanism proposed in Fig. 1b.

The electron is the catalyst for the molecular recognition between $\mathbf{R}^{2(\bullet+)}$ and $\mathbf{D}^{+(\bullet+)}$, whereas $CoCp_2$ serves only as a chemical electron source and an initiator of the process. A corollary[17] to this mechanistic insight is that any chemical reagents with (1) appropriate reduction potentials to transform $BIPY^{\bullet+}$ into $BIPY^{(0)}$ and (2) reasonable electron-transfer rates can, in principle, initiate the electron catalysis. Hence, we have screened a variety of chemical reagents, including active metals, metal complexes and organic reductants, and demonstrated their effectiveness (Supplementary Figs. 29–37) in promoting molecular recognition. This finding indicates that the strategy of electron catalysis is only weakly dependent on the structures of the chemical initiators, an observation that shows our approach is fundamentally different from previous strategies[13–15] that rely on elaborately designed catalysts.

The mechanistic understanding of electron catalysis prompted us to control the molecular recognition by electrochemical means, which is a clean and straightforward way to inject electrons. When we perform electrolysis on the mixture of $\mathbf{R}^{2(\bullet+)}$ and $\mathbf{D}^{+(\bullet+)}$ in an undivided cell, the simultaneous cathodic reduction and anodic oxidation of $BIPY^{\bullet+}$ radical cations are expected to occur, generating equal amounts of $BIPY^{(0)}$

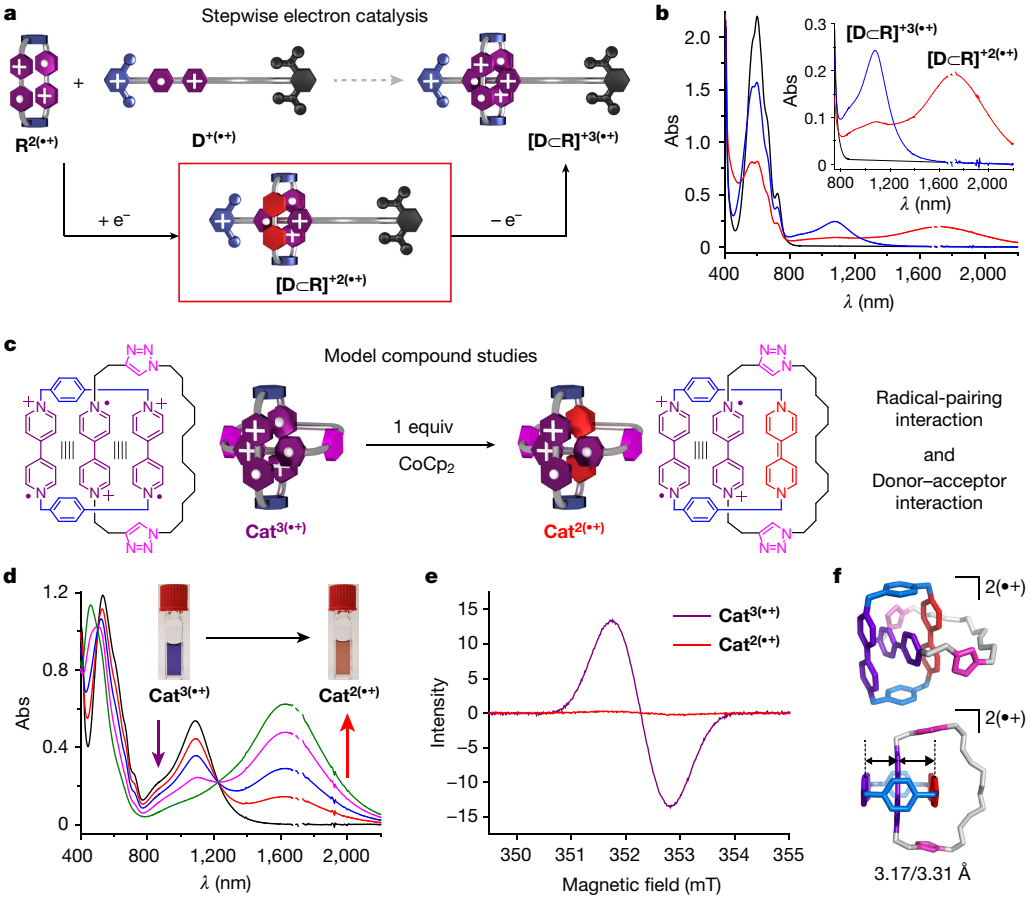

Fig. 3 | Detection and verification of the key intermediate in the electron-catalysed molecular recognition process. a, **b**, A stepwise electron catalysis monitored by UV/Vis/NIR spectroscopy. Initial state: molecular recognition between $\mathbf{R}^{2(\bullet+)}$ and $\mathbf{D}^{+(\bullet+)}$ occurs to a negligible extent (the black line in **b**). Electron injection: 1 equiv of $CoCp_2$ was introduced into the system, leading to the formation of the $[\mathbf{D}\subset\mathbf{R}]^{+2(\bullet+)}$ bisradical complex (the red line in **b**). Electron removal: excess of either $\mathbf{R}^{2(\bullet+)}$ or $\mathbf{D}^{+(\bullet+)}$ was introduced to oxidize the bisradical complex to the $[\mathbf{D}\subset\mathbf{R}]^{+3(\bullet+)}$ trisradical complex (the blue line in **b**). **c**–**f**, Investigation of a [2]catenane ($\mathbf{Cat}^{6+}$) model compound, focusing on its bisradical dicationic state, $\mathbf{Cat}^{2(\bullet+)}$. **c**, Combined structural formulae and graphical representation of the quantitative transformation from $\mathbf{Cat}^{3(\bullet+)}$ to $\mathbf{Cat}^{2(\bullet+)}$ using 1 equiv of $CoCp_2$. **d**, Evolution of UV/Vis/NIR spectra during the titration with $CoCp_2$, and photographs showing the colour change in the MeCN solution as $\mathbf{Cat}^{3(\bullet+)}$ is reduced to $\mathbf{Cat}^{2(\bullet+)}$. The discontinuities in the spectra at around 1,700 nm result from the cropping out of the sharp solvent peaks to present clearly the absorption of $\mathbf{Cat}^{2(\bullet+)}$. **e**, Electron paramagnetic resonance spectra of $\mathbf{Cat}^{3(\bullet+)}$ and $\mathbf{Cat}^{2(\bullet+)}$ recorded in MeCN at room temperature. **f**, Single-crystal structure of $\mathbf{Cat}^{2(\bullet+)}$, with annotated centroid-to-centroid distances between adjacent $BIPY^{\bullet+/(0)}$ units. Hydrogen atoms are omitted for the sake of clarity.

and $BIPY^{2+}$, respectively. These changes in the redox state are transient, because a spontaneous, mass transport-controlled single-electron transfer (SET) between $BIPY^{(0)}$ and $BIPY^{2+}$ will restore $BIPY^{\bullet+}$. We surmise that if the lifetime of $BIPY^{(0)}$ and $BIPY^{2+}$ is sufficiently longer than the time required for molecular recognition, then the injection and removal of electrons at the electrodes can promote the complexation between $\mathbf{R}^{2(\bullet+)}$ and $\mathbf{D}^{+(\bullet+)}$ in solution.

As both $\mathbf{R}^{2(\bullet+)}$ and $\mathbf{D}^{+(\bullet+)}$ contain $BIPY^{\bullet+}$ radical cations that can accept/lose electrons from/to the electrode, there are several possible pathways for molecular recognition to occur during the electrochemical process. Figure 4a illustrates one of the possibilities in which the cathodic reduction and anodic oxidation are both imposed on $\mathbf{R}^{2(\bullet+)}$, generating equal amounts of $\mathbf{R}^{\bullet+}$ and $\mathbf{R}^{2+(\bullet+)}$, respectively. After the electrochemical initiation, some of the $\mathbf{R}^{\bullet+}$ can bind rapidly with $\mathbf{D}^{+(\bullet+)}$, leading to the formation of the $[\mathbf{D}\subset\mathbf{R}]^{+2(\bullet+)}$ bisradical complex. Subsequently, this intermediate can undergo SET with $\mathbf{R}^{2(\bullet+)}$, producing a $[\mathbf{D}\subset\mathbf{R}]^{+3(\bullet+)}$ trisradical complex as the final product and generating a new $\mathbf{R}^{\bullet+}$ to restart the cycle (propagation). The catalytic cycle is terminated when the $[\mathbf{D}\subset\mathbf{R}]^{+2(\bullet+)}$ bisradical complex undergoes SET with $\mathbf{R}^{2+(\bullet+)}$ to recover $\mathbf{R}^{2(\bullet+)}$ as the starting material or transfers an electron back (BET) to the anode and generates a $[\mathbf{D}\subset\mathbf{R}]^{+3(\bullet+)}$ trisradical complex. Several other possible pathways, following similar logic, are illustrated in Supplementary Figs. 41–43. During the electrolysis under stirring, the number of catalytic cycles before termination depends on the convection rates of the intermediates. Detailed discussions regarding theoretical analyses of electrochemically controlled molecular recognition can be found in the Supplementary Information.

To validate the proposed electrochemical mechanism, the electrolysis of a MeCN solution containing $\mathbf{R}^{2(\bullet+)}$ and $\mathbf{D}^{+(\bullet+)}$ was conducted at a constant current and stirring rate under a N_2 atmosphere, followed by the periodical sampling of the solution to record the UV/Vis/NIR spectrum. After the first 3 min of electrolysis, we observed (Fig. 4b, c and Supplementary Figs. 44 and 45) an increase in the absorption band characteristic of the $[\mathbf{D}\subset\mathbf{R}]^{+3(\bullet+)}$ trisradical complex. The measurement of the same sample, after it was maintained in the spectrometer for 3 min, revealed that the absorbance underwent no change. Repeated on/off cycling of electricity results in the intermittent increase in the formation of trisradical complexes. These observations have demonstrated[23] a rare example of temporally controlled supramolecular processes, enabling us to produce kinetically stable systems[24] with well-defined distributions between substrates and complexes; that is, by applying electricity for a pre-determined time, we can create a system with a molar ratio between substrates and complexes ranging anywhere between zero and the equilibrium value. In contrast with the

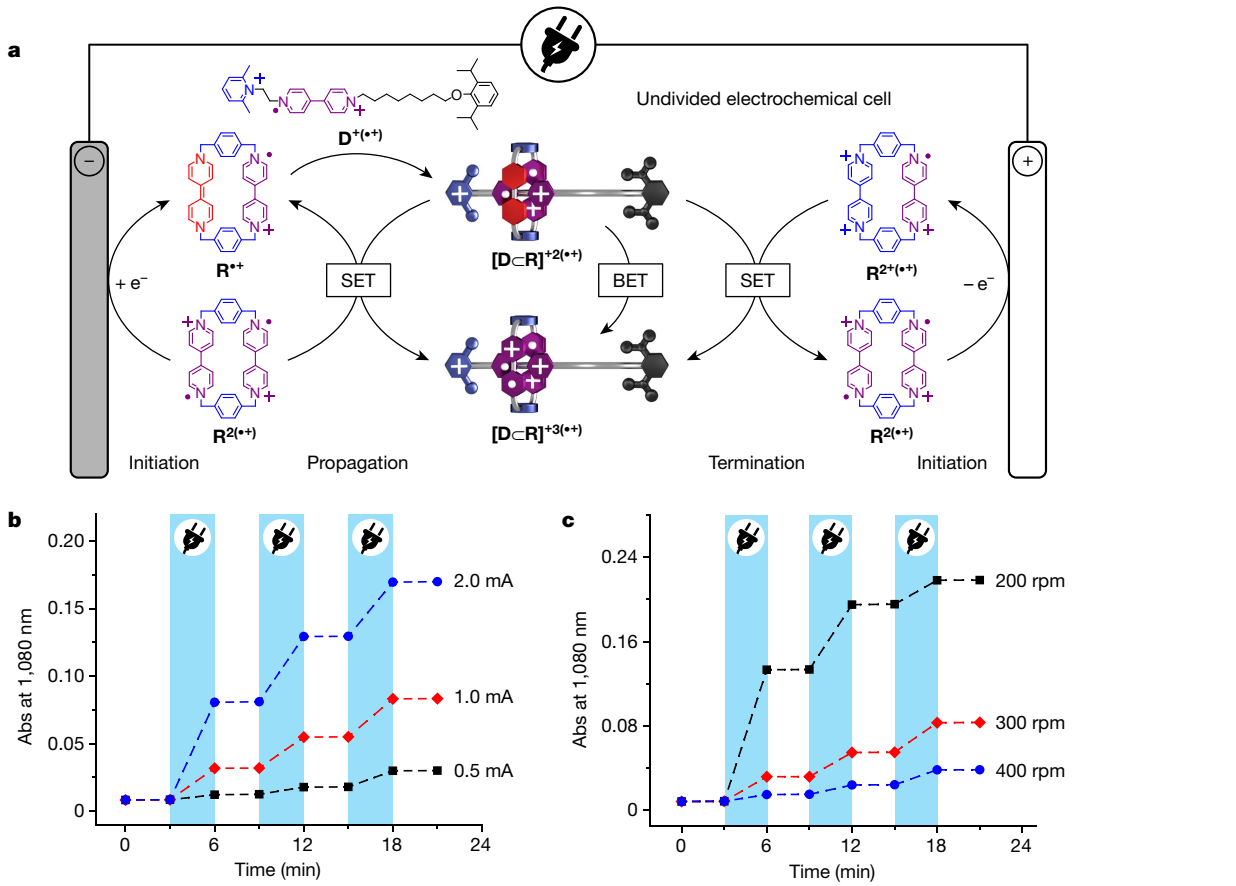

Fig. 4 | Electrochemically controlled molecular recognition. a, A combined structural formulae and graphical representation of one of the possible pathways involving molecular recognition during the electrolysis in an undivided cell. The overall process is composed of three stages. Stage 1, initiation: on applying electricity, one $BIPY^{\bullet+}$ unit in an $\mathbf{R}^{2(\bullet+)}$ is reduced to $BIPY^{(0)}$ at the cathode. Concurrently, one $BIPY^{\bullet+}$ unit in another $\mathbf{R}^{2(\bullet+)}$ is oxidized to $BIPY^{2+}$ at the anode. Stage 2, propagation: the resulting $\mathbf{R}^{\bullet+}$ binds rapidly with $\mathbf{D}^{+(\bullet+)}$ to form a $\mathbf{[D{\subset}R]}^{+2(\bullet+)}$ bisradical complex. This intermediate undergoes single-electron transfer (SET) with $\mathbf{R}^{2(\bullet+)}$, producing a $\mathbf{[D{\subset}R]}^{+3(\bullet+)}$ trisradical complex as the final product and generating a new $\mathbf{R}^{\bullet+}$ to restart the cycle. Stage 3, termination: the $\mathbf{[D{\subset}R]}^{+2(\bullet+)}$ bisradical complex transfers an electron to $\mathbf{R}^{2+(\bullet+)}$, recovering $\mathbf{R}^{2(\bullet+)}$ as the starting material, or undergoes a back electron transfer (BET) to the anode and generates a $\mathbf{[D{\subset}R]}^{+3(\bullet+)}$ trisradical complex. **b**, **c**, Changes in the absorbance at 1,080 nm during the intermittent electrolysis of the mixture of $\mathbf{R}^{2(\bullet+)}$ and $\mathbf{D}^{+(\bullet+)}$ under different conditions. **b**, The stirring rate was fixed at 300 rpm and the current intensity was set to be 0.5, 1.0 and 2.0 mA. **c**, The current intensity was fixed at 1.0 mA and the stirring rate was set to be 200, 300 and 400 rpm. Credit for electric plug icon: Pavlo Stavnichuk / iStock / Getty images.

chemical addition of electrons that cannot be removed simultaneously, the electrolysis in an undivided cell enables molecular recognition to be controlled temporally because of the constant delivery of anodically formed oxidants that curb the propagation of catalytic cycles and quench the molecular recognition after the electricity is switched off.

In addition to the temporal control, the kinetics of molecular recognition is tuneable by adjusting the working conditions of the electrolysis, such as current intensity and stirring rate. On the one hand, increasing the current from 0.5 to 1.0 to 2.0 mA—with the same stirring rate at 300 rpm—gives rise to an increased speed (Fig. 4b) in molecular recognition. On the other hand, comparison (Fig. 4c) between the kinetic traces at 200, 300 and 400 rpm stirring rate—with fixed current at 1.0 mA—reveals that molecular recognition is slowed down when stirring the solution more vigorously. A plausible reason for this observation is that, in an undivided cell, faster convection will expedite SET between $BIPY^{(0)}$ and $BIPY^{2+}$ and thus decrease the lifetime of both species, given the consideration that the $BIPY^{(0)}$ unit is responsible for facilitating molecular recognition. In short, extending the paradigm of electron catalysis from synthetic covalent chemistry to supramolecular non-covalent chemistry unleashes the tremendous power of the electron in promoting and controlling self-assembly processes.

Online content

Any methods, additional references, Nature Research reporting summaries, source data, extended data, supplementary information, acknowledgements, peer review information; details of author contributions and competing interests; and statements of data and code availability are available at https://doi.org/10.1038/s41586-021-04377-3.

1. Lehn, J.-M. Supramolecular chemistry—Scope and perspectives. Molecules, supermolecules, and molecular devices (Nobel lecture). *Angew. Chem. Int. Ed. Engl.* **27**, 89–112 (1988).
2. Cram, D. J. The design of molecular hosts, guests, and their complexes (Nobel lecture). *Angew. Chem. Int. Ed. Engl.* **27**, 1009–1020 (1988).
3. Philp, D. & Stoddart, J. F. Self-assembly in natural and unnatural systems. *Angew. Chem. Int. Ed. Engl.* **35**, 1154–1196 (1996).
4. Persch, E., Dumele, O. & Diederich, F. Molecular recognition in chemical and biological systems. *Angew. Chem. Int. Ed.* **54**, 3290–3327 (2015).
5. Aida, T., Meijer, E. W. & Stupp, S. I. Functional supramolecular polymers. *Science* **335**, 813–817 (2012).
6. Das, K., Gabrielli, L. & Prins, L. J. Chemically fueled self-assembly in biology and chemistry. *Angew. Chem. Int. Ed.* **60**, 20120–20143 (2021).
7. Weißenfels, M., Gemen, J. & Klajn, R. Dissipative self-assembly: fueling with chemicals versus light. *Chem* **7**, 23–37 (2021).
8. Yin, Z. et al. Dissipative supramolecular polymerization powered by light. *CCS Chem.* **1**, 335–342 (2019).
9. Wiester, M. J., Ulmann, P. A. & Mirkin, C. A. Enzyme mimics based upon supramolecular coordination chemistry. *Angew. Chem. Int. Ed.* **50**, 114–137 (2010).

10. Webber, M. J., Appel, E. A., Meijer, E. W. & Langer, R. Supramolecular biomaterials. *Nat. Mater.* **15**, 13–26 (2015).
11. Amabilino, D. B., Smith, D. K. & Steed, J. W. Supramolecular materials. *Chem. Soc. Rev.* **46**, 2404–2420 (2017).
12. Wang, Y. et al. What molecular assembly can learn from catalytic chemistry. *Chem. Soc. Rev.* **43**, 399–411 (2014).
13. Turberfield, A. J. et al. DNA fuel for free-running nanomachines. *Phys. Rev. Lett.* **90**, 118102 (2003).
14. Zhang, D. Y., Turberfield, A. J., Yurke, B. & Winfree, E. Engineering entropy-driven reactions and networks catalyzed by DNA. *Science* **318**, 1121–1125 (2007).
15. Song, T. & Liang, H. Synchronized assembly of gold nanoparticles driven by a dynamic DNA-fueled molecular machine. *J. Am. Chem. Soc.* **134**, 10803–10806 (2012).
16. Li, H. et al. Proton-assisted self-assemblies of linear di-pyridyl polyaromatic molecules at solid/liquid interface. *J. Phys. Chem. C* **116**, 21753–21761 (2012).
17. Studer, A. & Curran, D. P. The electron is a catalyst. *Nat. Chem.* **6**, 765–773 (2014).
18. Francke, R. & Little, R. D. Electrons and holes as catalysts in organic electrosynthesis. *ChemElectroChem* **6**, 4373–4382 (2019).
19. Yan, M., Kawamata, Y. & Baran, P. S. Synthetic organic electrochemical methods since 2000: on the verge of a renaissance. *Chem. Rev.* **117**, 13230–13319 (2017).
20. Prier, C. K., Rankic, D. A. & MacMillan, D. W. C. Visible light photoredox catalysis with transition metal complexes: applications in organic synthesis. *Chem. Rev.* **113**, 5322–5363 (2013).
21. Romero, N. A. & Nicewicz, D. A. Organic photoredox catalysis. *Chem. Rev.* **116**, 10075–10166 (2016).
22. Trabolsi, A. et al. Radically enhanced molecular recognition. *Nat. Chem.* **2**, 42–49 (2010).
23. Aubert, S., Bezagu, M., Spivey, A. C. & Arseniyadis, S. Spatial and temporal control of chemical processes. *Nat. Rev. Chem.* **3**, 706–722 (2019).
24. Mattia, E. & Otto, S. Supramolecular systems chemistry. *Nat. Nanotechnol.* **10**, 111–119 (2015).
25. Whitesides, G. M. Self-assembly at all scales. *Science* **295**, 2418–2421 (2002).
26. Harada, A., Kobayashi, R., Takashima, Y., Hashidzume, A. & Yamaguchi, H. Macroscopic self-assembly through molecular recognition. *Nat. Chem.* **3**, 34–37 (2010).
27. Santos, P. J., Gabrys, P. A., Zornberg, L. Z., Lee, M. S. & Macfarlane, R. J. Macroscopic materials assembled from nanoparticle superlattices. *Nature* **591**, 586–591 (2021).
28. Lehn, J. M. Toward self-organization and complex matter. *Science* **295**, 2400–2403 (2002).
29. Vantomme, G. & Meijer, E. W. The construction of supramolecular systems. *Science* **363**, 1396–1397 (2019).
30. Pezzato, C., Cheng, C., Stoddart, J. F. & Astumian, R. D. Mastering the non-equilibrium assembly and operation of molecular machines. *Chem. Soc. Rev.* **46**, 5491–5507 (2017).
31. Luca, O. R., Gustafson, J. L., Maddox, S. M., Fenwick, A. Q. & Smith, D. C. Catalysis by electrons and holes: formal potential scales and preparative organic electrochemistry. *Org. Chem. Front.* **2**, 823–848 (2015).
32. Whitesides, G. M. et al. Noncovalent synthesis: using physical-organic chemistry to make aggregates. *Acc. Chem. Res.* **28**, 37–44 (1995).
33. Reinhoudt, D. N. Synthesis beyond the molecule. *Science* **295**, 2403–2407 (2002).
34. Frasconi, M. et al. Redox control of the binding modes of an organic receptor. *J. Am. Chem. Soc.* **137**, 11057–11068 (2015).
35. Wang, Y. et al. Symbiotic control in mechanical bond formation. *Angew. Chem. Int. Ed.* **55**, 12387–12392 (2016).
36. Cai, K. et al. Molecular Russian dolls. *Nat. Commun.* **9**, 5275 (2018).

Methods

General methods for conducting chemically initiated molecular recognition

Homogenous chemical initiators. A screw-cap cuvette was charged with MeCN solutions of $\mathbf{R}^{2(\bullet+)}$ (0.3 mM, 500 µl, 1 equiv) and $\mathbf{D}^{+(\bullet+)}$ (0.3 mM, 500 µl, 1 equiv) in a N_2-filled glovebox. A specific amount of chemical initiator (for example, a MeCN solution of $CoCp_2$ (1.5 mM, 4 µl, 4 mol%)) was added to the system. After rapid mixing of the solution, the sealed cuvette was transferred to a spectrometer and the UV/Vis/NIR spectra were recorded at 2-min intervals. The kinetic trace of this process was obtained by plotting the absorbance at 1,080 nm against time.

Heterogenous chemical initiators. MeCN solutions of $\mathbf{R}^{2(\bullet+)}$ (0.3 mM, 500 µl, 1 equiv) and $\mathbf{D}^{+(\bullet+)}$ (0.3 mM, 500 µl, 1 equiv) were combined in a vial, followed by the addition of excess of metal (for example, Zn) dust. The suspension was stirred in a N_2-filled glovebox for 20 min. After removing the solid by filtration, the resulting solution was transferred to a screw-cap cuvette to record the UV/Vis/NIR spectra.

General methods for conducting electrochemically controlled molecular recognition

Electrochemically controlled molecular recognition between $\mathbf{R}^{2(\bullet+)}$ and $\mathbf{D}^{+(\bullet+)}$ was conducted in the N_2-filled glovebox using an IKA Electrasyn 2.0 Device. The set-up was an undivided electrochemical cell, in which both the cathode and anode are reticular vitreous carbon electrodes. In a typical procedure, a MeCN solution (9 ml) containing $\mathbf{R}^{2(\bullet+)}$ (0.15 mM), $\mathbf{D}^{+(\bullet+)}$ (0.15 mM) and tetrabutylammonium hexafluorophosphate ($TBAPF_6$, 0.05 M) was electrolysed for 3 min at a constant current (for example, 1.0 mA) and stirring rate (for example, 300 rpm). Subsequently, the current was switched off and the solution was allowed to stand for 3 min. The overall process consisted of three on/off cycles. The molecular recognition during the intermittent electrolysis was monitored by sampling the solution at 3-min intervals and recording its UV/Vis/NIR spectra.

Data availability

The data that support the findings of this study are available within the paper and its Supplementary Information files.

Acknowledgements We thank Northwestern University (NU) for its continued support of this research and acknowledge the Integrated Molecular Structure Education and Research Center (IMSERC) at NU for providing access to equipment for relevant experiments. The computational investigations at California Institute of Technology were supported by National Science Foundation grant no. CBET-2005250 (W.-G.L. and W.A.G.). This work was also supported by the Department of Energy, Office of Science, Office of Basic Energy Sciences under Award DE-FG02-99ER14999 (M.R.W.) and the Natural Science Foundation of Anhui Province grant no. 2108085MB31 (D.S.).

Author contributions Y.J., Y.Q. and J.F.S. conceived the idea for this project. L.Z. proposed a key mechanistic conjecture. W.-G.L. and W.A.G. performed quantum mechanical calculations. Y.J. and Y.Q. synthesized and characterized the materials with the help of H.C., Y.F., K.C., D.S., B.S., X.-Y.C., X.L. and X.Z. H.M., R.M.Y. and M.R.W. performed the electron paramagnetic resonance characterizations and detailed analyses. C.L.S. performed the single-crystal X-ray diffraction. R.D.A. contributed to the theoretical analyses on the mechanism of electron catalysis. Y.J., Y.Q. and J.F.S. wrote the first and second drafts of the paper. J.F.S. and W.A.G. directed the project. All the authors participated in evaluating the results and commented on the manuscript.

Competing interests Y.J., Y.Q. and J.F.S. have filed a patent application lodged with Northwestern University (INVO reference no. NU 2021-248) based on this work.

Additional information
Supplementary information The online version contains supplementary material available at https://doi.org/10.1038/s41586-021-04377-3.
Correspondence and requests for materials should be addressed to William A. Goddard III or J. Fraser Stoddart.
Peer review information *Nature* thanks Robert Francke and the other, anonymous, reviewer(s) for their contribution to the peer review of this work. Peer reviewer reports are available.

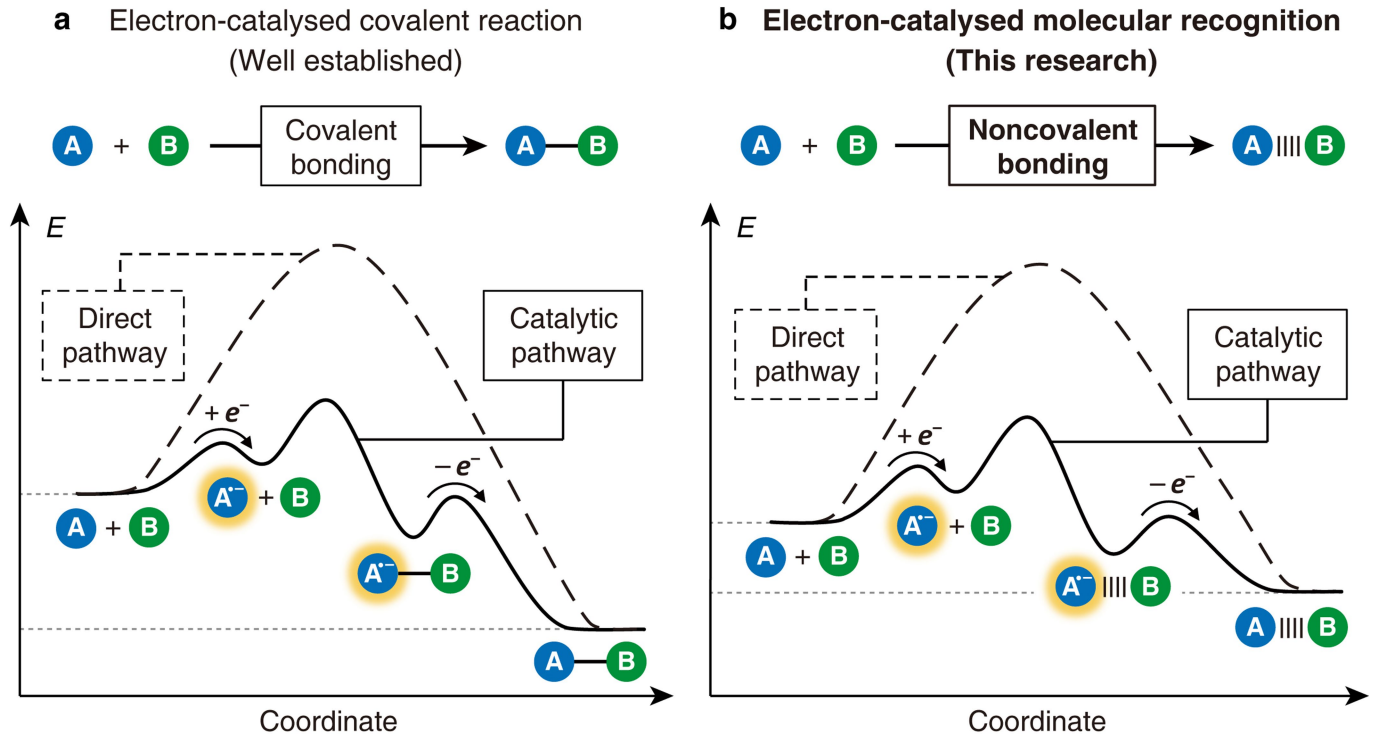

Extended Data Fig. 1 | The electron as an efficient catalyst for both covalent reactions and molecular recognition. a, Electron-catalysed covalent reactions are well established in synthetic covalent chemistry, particularly for radical-mediated photoredox catalysis and organic electrosynthesis. Consider a reaction **A** + **B** → **A**–**B**, where a high energy barrier causes the reaction to be very slow. Injection of an electron reduces one of the substrates (**A**) to a highly reactive radical species (**A**$^{\bullet-}$), which can rapidly form a covalent bond with the other substrate (**B**). The resulting intermediate (**A**$^{\bullet-}$–**B**) releases the electron to afford the final product (**A**–**B**). Whereas the overall process is redox neutral, i.e., the redox state remains the same during the transformation from the substrates to product, the catalytic pathway, which involves the temporary addition of an electron, leads to a substantially lower energy barrier, thereby expediting the formation of the covalent bond. In this process, the electron has acted as an effective catalyst. **b**, The research reported in this article aims to extend the paradigm of electron catalysis to promoting and controlling molecular recognition. The trajectory for this noncovalent process is similar to that for electron-catalysed covalent reactions, except that the product is a supramolecular complex wherein molecular components are assembled courtesy of noncovalent bonding interaction(s), rather than a molecule whose atoms are connected by covalent bond(s).